Air core inductors study for DC/DC power supply in harsh radiation environment.

S. Michelis[a,b], F. Faccio[a], P. Jarron[a], M. Kayal[b]
[a] CERN (European Organization for Nuclear Research), Geneva, Switzerland
[b] Electrical Engineering Institute, EPFL (Ecole Polytechnique Federale de Lausanne), Switzerland

***Abstract*— In high energy physics and space applications it becomes mandatory to solve specific problems concerning the power supply. In both cases, it exists a harsh radiation environment and the presence of external electromagnetic perturbations. The former prevents the use of standard technology and many studies on this subject were already made. Solutions foresee the use of ad-hoc technologies or the modification of the layout of standard technologies. The latter causes problems concerning the magnetic elements used in many switching power supply topology.**

The aim of this study is the analysis of the magnetic components necessary in these circuits, their environmental constrains and their evaluations through simulations and practical tests in order to show up which geometry is preferable to limit injection of noise and to increase the efficiency.

***Index Terms*— Power Management, DC-DC converter, Air-core Inductors, High Energy Physics.**

I. Introduction

HIGH energy physics experiments requires dedicated instruments that are accelerators and detectors. Accelerators are used to accelerate beams of charged particles that collide with another bunch of particles coming from the opposite direction or hit a fixed target. At CERN a new accelerator is going to be completed ant its name is LHC (Large Hadron Collider). A detector is built around the collision point in order to study the products of the collision. In this paper, the detector and its infrastructure are called experiment. A part of the detector is surrounded by an electromagnet (generally with superconducting coils) which generates a very strong magnetic flux density (up to 4 T), used to bend the charged particle's trajectory. From the curvature, it is possible to extract the momentum and the charge sign (polarity). In the LHC experiments, due to the collisions of the particles, very high background radiation levels will be obtained, especially in the sub-detectors closer to the particle interaction point. Therefore, all the electronics that operate inside the detectors have to work in an extremely harsh environment because of high magnetic flux density and high level of radiation.

Manuscript submitted on January 14, 2008. This work was supported by the CERN (European Organization for Nuclear Research), Geneva, Switzerland and by the EPFL (Ecole Polytechnique Federale de Lausanne), Lausanne, Switzerland under the Sponsorship of the EP7 Marie Curie Early Stage Training.

S. Michelis is with the CERN and he is pursuing his PhD thesis at EPFL (phone: 0041227675824; e-mail: stefano.michelis@cern.ch)

F. Faccio and P. Jarron are with the CERN, Geneva, Switzerland (e-mail: federico.faccio@cern.ch, pierre.jarron@cern.ch).

M. Kayal. is with the Electrical Engineering Department, EPFL, Lausanne, Switzerland (e-mail: maher.kayal@epfl.ch).

II. Power Distribution Scheme

The distribution of power in LHC experiments faces difficult engineering challenge, given the global requirements in terms of power needs, available cooling capacity and limited material budget. The harsh radiation environment and the intense magnetic field make conventional switching converters unusable in many locations. Therefore, the actual LHC's experiments distribution scheme foresees power suppliers outside the detector as it is possible to see in Fig. 1 [1][2][4][5][6].

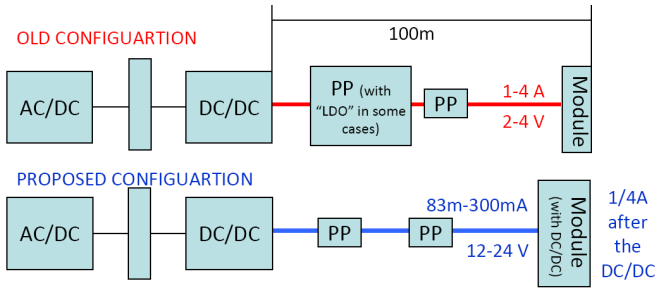

Fig. 1 Power supply schemes (old and new configuration)

The front-end circuits are connected with long cables (up to 100m) that do not guarantee a stable input voltage (2-4V) and dissipate power in heat, increasing the cooling system's load. In the same case, linear regulators [7][8] are placed on patch panels (PP) to stabilize the input voltage. The power needed by the actual modules is around 6W. In view of LHC upgrades where front-end circuits might require even larger supply currents at low voltage (total power needed will be more than 20W), it is necessary to evaluate an alternative power distribution scheme. This could be based on the distribution of higher voltage (12-24 V) from external power supplies to custom made radiation-hard converters capable of resisting to high magnetic field, installed locally inside the detectors. They will then convert the power to the low voltage (2-4V) and high current (1/4A) required by the front-end circuitry. In this contest, we are developing an inductor based switching DC-DC step-down converter.

III. DC/DC Architecture

Inductor based step-down converters comprise mainly a magnetic component, some switches, an output capacitor and control circuit (a schematic illustration of a converter is shown in Fig.1 and its name is buck converter).

978-1-4244-2332-3/08/$25.00 © 2008 IEEE

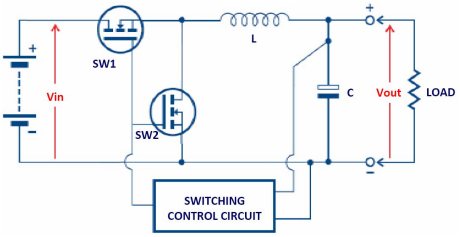

Fig. 2 Basic step-down (buck) converter.

The two transistors are directly connected to the input voltage (12 - 24 V) so they need to have be able to support such voltage on the V_{DS}. So a 0.35 µm CMOS technology usually employed in automotive applications was selected for the design of the switches and the control circuit because the transistors of this technology can stand up to a V_{DS} of 80V on their drain. Devices with a modified layout inspired from [9][10] used in low voltage CMOS technologies to enhance radiation tolerance were designed and tested. As shown in Figure 3 the modification of the layout eliminates the source of leakage current and only a residual increase of leakage due to a decrease in V_{th} and increase of the subthreshold swing (from 86 mV/dec to 92 mV/dec) is observed. Threshold voltage shift is limited to about -40mV in all conditions for the range of TID explored.

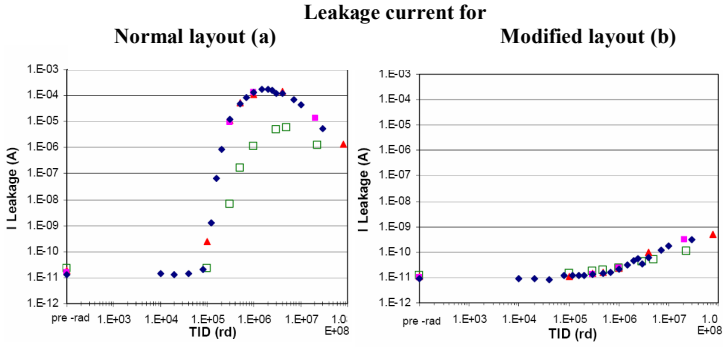

Fig. 3 Evolution of the leakage current for NMOS transistors (4 different chips) with standard (a) and modified (b) layout.

The switches were dimensioned in order to have a good balance between switching and conducting losses [15]. Additionally their area is limited by yield-related considerations. Given the large current flowing (up to 4 A) its layout has to be carefully studied to minimize the resistance between input and output pads. The gate driving signal distribution is also critical.

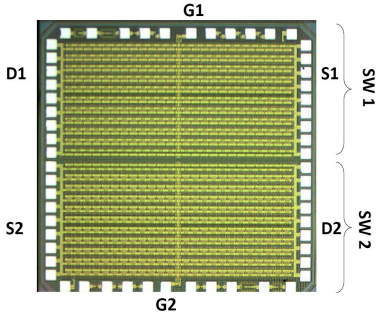

Fig. 4 layout of the two switches with W=0,1m

These power devices are vertical MOS and the only free parameter is the W. With a W of 0.1m the on-resistance is equal to 330mOhm and the total gate capacitance is 1nF. In order to realize such big transistor we use multiple unit cells, each with a number of fingers to have the required total W. This allows a more uniform distribution of the current over the different cells, hence a more efficient use of each cell. It also has the benefit that many more drain contacts are available, which improves the possibilities for routing and increases substantially the yield of the circuit. In Fig.4 the layout of the two switches is presented. The total area is around 4mm^2.

IV. Inductors Issues

The magnetic elements within a switching power supply play a cornerstone role in its operation. In this paper, studies and results on different shaped inductors will be presented, focusing the attention on the emitted magnetic field, on the series resistance that influence the efficiency of the converter and on the mass of metal required to create the inductor. Limitation of mass is required for better particle measures. The very high external magnetic flux density (up to 4 T) strongly limits the choice of the inductor because it prevents the possibility to use magnetic cores. This is due to the saturation of all ferromagnetic materials. In Table I. some ferromagnetic materials with high value of saturation flux density are shown [11]. Ferromagnetic materials as permendur and iron can reach values of saturation flux density around 2 T but at 4 T all the magnetic domains align their dominant magnetic orientation in the direction of the applied magnetic field. In this case the core can make no further contribution to flux growth and any increase thereafter is limited to that provided by the air permeability. Therefore, it is necessary to use an air core inductor in order to avoid any problem of magnetic saturation of the core and obtain an inductor whose value does not depend on the external magnetic field.

TABLE I. Permeability (µ) and Saturation Flux Density of Magnetic Materials

Material	µ at B=2mT	Max. µ	SatB(T)
Cold rolled steel	180	2,000	2,1
Iron	200	5,000	2,15
Purified iron	5,000	180,000	2,15
4% Silicon-iron	1,500	30,000	2,0
Permendur	800	5,000	2,45
2V Permendur	800	4,500	2,4
Hiperco	650	10,000	2,42

Without a high permeability core it is necessary to have higher length to achieve a given inductance value, increasing in a substantial way the volume. More turns means larger coils, lower self-resonance and higher copper loss. The air core inductors produce a reduction of the efficiency of the system due to its parasitic resistance in comparison to an inductor with a ferromagnetic core. This also limits the choice of the architecture for inductor based switching converter. Without ferromagnetic cores, transformers would have excessive losses; this implies that isolating converter topologies cannot be used.

In addition to all these issues, we have to consider that in a ferromagnetic core works as a collector of the flux, concentrating the magnetic field around and inside the inductor. In that way the magnetic field lines are well confined inside a definite volume. In this specific application with switching current inside the air core inductor, an AC magnetic field will be generated introducing noise in neighbouring

electronics. This can disturb the very sensitive front-end electronics. To know the noise introduced it is necessary to study the spatial distribution of such a magnetic field.

In this paper simulations will be presented for different shaped inductor to limit as much as possible the injected noise. Air core inductors with an inductance value between 500nH and 1µH are foreseen as a good trade-off.

V. Design Methodology of the Air Core Inductors

Three inductors shape are studied in this paper: a solenoid (a cylindrical coil), a toroid and a planar inductor. The last one is designed to be implemented on a PCB.

The calculation of the inductances of cylindrical and toroidal coil is dictated respectively by the following formula:

$$L_{solenoid} = \mu_0 \mu_r \frac{N^2 A}{l} \quad \text{and} \quad L_{toroid} = \mu_0 \mu_r \frac{N^2 r^2}{D}$$

where L = inductance in henries (H), μ_0 = permeability of free space = $4\pi \times 10\text{-}7$ H/m, µr = relative permeability of core material, N = number of turns, A = area of cross-section of the coil in square meters (m^2), l = length of coil in meters (m), r = radius of coil winding (m) and D = overall diameter of toroid (m). For air core inductor μ_r=1.

With r=2mm, l=28mm, N=32 turns, D=9mm it results that $L_{solenoid}$=577nH and L_{toroid}=571nH. Using in both cases a copper wire with thickness of 0,25mm the DC series resistance is around 35mΩ. The total metal volume is 12 mm^3.

For what concerns the planar inductor [12][13][14] the formula used to calculate the inductance is:

$$L_T = l + \sum m$$

Where L_T is the total inductance, is the sum of the self-inductance of all the straight segments and $\sum m$ is the sum of all the mutual inductances, both positive and negative. Mutual inductance is positive when current flow in two parallel conductors in the same direction and negative when current flow is in opposite directions. In asymmetrical spiral inductor shown in figure 5.a mutual contributes negatively to inductance. In the case of symmetrical spiral inductor shown in figure 5.b mutual inductance is additive to self inductance maximizing inductance value for a given wire length and series resistance

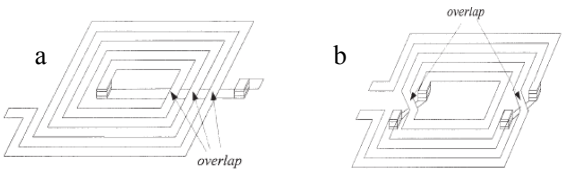

Fig. 5 Layouts of a asymmetrical spiral inductor (a) and of a square spiral symmetrical inductor (b)

A variant octagonal layout shape is even better providing the same total inductance with 90 % of the wire length, which minimize series resistance. With symmetrical spiral inductor layout, the approximate inductance is $L_T \approx 2.7 l_{tot}$ with L_T in nH, l_{tot} (the total length of the inductor) in mm, width strip (w) 0.4mm and a spacing between turns (s) of 0.2 mm. Assuming octagons have circle perimeter, hence:

$$\ell_{tot} \approx \pi \sum_{1}^{N} \tfrac{1}{2} n(n+1) + n.ID \quad \text{and} \quad OD \approx ID + (s+w)N$$

with N the number of turns, ID the inner diameter and OD the outer diameter. Using N=8, ID= 6mm it results that l_{tot} is around 336mm and OD=16,7 mm. Then L_T=940nH.

The DC resistance is 200mΩ with 70µm thick PCB copper layer. In this calculation VIA resistance is neglected. Tests on real spiral inductors show that the DC resistance is around 270 mΩ. The total metal volume is 9.4 mm^3.

The designed inductors are shown in Fig. 6.

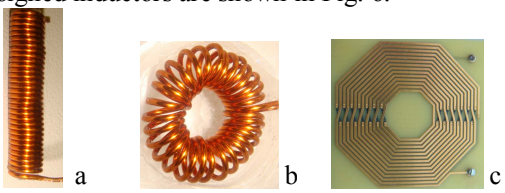

Fig. 6 Solenoidal (a), toroidal (b), planar (c) inductors

VI. Simulation Results

A. Simulation details

Ansoft Maxwell was used for simulations. The inductors are made with copper and put in an air environment. The current is set at 1A. The simulation is static because dynamic simulations would require a too long execution time with our computers and because we are interested on the maximum magnetic field emitted by the peak current (1A).

B. Simulation results

All the results presented are in form of figures taken after the simulations. Each figure has its own scale, in order to better visualize how much the generated magnetic field is extended in space. In the plots, all the magnetic field values that are bigger than the maximum are represented by the same color of the maximum (red). Some arrows will indicate the space dimensions. The three inductors are in scale between them the picture. With a scale 1µT – 10µT (Fig 7) we can appreciate that magnetic field emitted extends far from the inductors in different ways. For the cylindrical inductor (Fig 7.a) we can sense a magnetic field of 1 µT at a distance of 36mm (a circumference with a diameter of 76mm). The spiral inductor (Fig 7.c) represents the worst case because the emission is comparable to a sphere with a diameter of 98mm.

These simulations show that the toroid (Fig 6.b) can reduce the emission of magnetic field because it is well confined in the inner part of the coil. This is because of the field's lines can be closed inside the inductor and not outside as in the case of the cylinder. The spatial emission is higher in the case of planar inductor in comparison with the solenoid or toroid inductor because the magnetic field is less confined inside the coils. This drawback is the cost to pay to avoid the presence of a PCB external inductor. It is necessary to say that in both cases the magnetic field emitted outside the inductor, with a 1A current, is generally in the order of µT at a distance of 5 cm, so the perturbation is very space-limited.

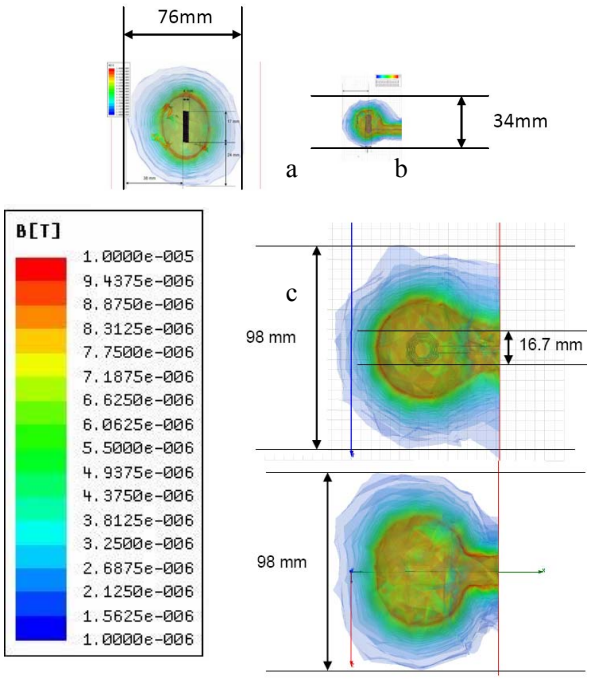

Fig. 7 Simulation results with scale 1μT -10μT for the solenoidal (a), toroidal (b), planar (c) inductors

VII. Inductors Implementation and Measurement Results

The designed inductors were implemented twisting copper cables for the solenoid and the toroid and a PCB layout was made for the spiral inductor.

Tests were made in order to measure the inductance and the quality factor (Q). The Q of an inductor is the ratio of its inductive reactance to its resistance at a given frequency, and is a measure of its efficiency. The higher the Q factor of the inductor, the closer it approaches the behavior of an ideal, lossless, inductor.

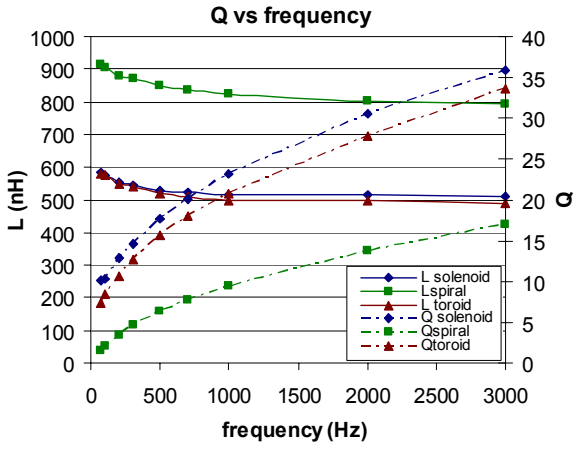

Fig. 8 L and Q vs frequency for the different inductors

In Fig 8 measures on the inductance and of the quality factor are shown. Practical values are closed to the calculated value during the design and comparable to the commercial devices. The toroid has lower Q than the solenoid because the winding it is not perfect. It results as well that the spiral inductor as a very low Q due to the high series resistance. The copper thickness of 70 μm strongly limits the efficiency of such inductor. If it would be possible to increase from 70 μm to 0.4mm the thickness of the copper , the spiral inductor could have the same DC resistance of the toroid and solenoid but with an higher value of inductance (940nH instead of 570nH).

The toroid and solenoid have a copper volume of around 79mm3 and in this case the planar inductor could have a volume of 54mm3. In conclusion, the spiral geometry with positive mutual inductance can provide higher L, Q and a reduction of the copper mass. It is necessary to make more studies on the feasibility on PCB or the use of wider path.

VIII. Conclusions

This paper shows that is possible to create a complete DC/DC converter for extremely harsh environment, such as the experiment of high-energy physics and space applications. Problems linked to this environment are solved with the optimization of the technology and the inductors. The technology can be radiation hardened with modifications of the layout and big power transistors can be designed and realized. A complete study, simulations and practical tests with different shaped inductors show that it is better to use a toroidal inductor for this specific application.

References

[1] S. Paoletti *et al.* "The Powering Scheme of the CMS Silicon Strip Tracker" 10th Workshop on electronics for LHC and future experiments, CERN 2004-010, CERN-LHCC- 2004-030 (2004).

[2] M. Costa *et al.* "Quality assurance for CMS Tracker LV and HV Power Supplies" 12thWorkshop on electronics for LHC and future experiments, CERN-2007-001, CERNLHCC 2007-006 (2007).

[3] S. Paoletti "The Implementation of the power supply system of the CMS Silicon Strip Tracker", *TWEPP-07,* Prague 2007

[4] R.D'Alessandro G. Parrini "Power Supply Implications (CMS Tracker)" CERN (30/08/2000) [Online].

[5] S. Kersten. (2000) Requirements for the power supply system of the ATLAS pixel detector, ATL-IP-ES-0005

[6] S. Kersten, P. Kind, S. K. Nderitu. (2004). The supply and control ystem for the Opto Link of the ATLAS pixel detector, ATL-IP-ES-0106.

[7] N. Boetti, F. Faccio, P. Jarron. (2000) A radiation hardened voltage regulator for LHC and space applications.

[8] M. Kayal, F. Vaucher and Phi. Deval,F. "New Error Amplifier Topology for Low Dropout Voltage Regulators Using Compound OTA-OPAMP". ESSCIRC'06, September 19 - 2006, Montreux, Switzerland.

[9] F. Faccio and G. Cervelli, "Radiation-induced edge effects in deep submicron CMOS transistors," *IEEE Transactions on Nuclear Science*, vol. 52, pp. 2413–2420, December 2005.

[10] G. Anelli, "Design and characterization of radiation tolerant integrated circuits in deep submicron CMOS technologies for the LHC experiments". PhD thesis, Insitut National Polytechnique de Grenoble, France, December 2000.

[11] B. Hansen. (2005). Magnetic materials [Online]. Available: http://www.oz.net/~coilgun/theory/materials.htm

[12] H. M. Greenhouse, "Design of Planar Rectangular Microelectronic Inductors,". *IEEE transactions on parts, hybrids, and packaging,* Volume 10, Issue 2, Jun 1974,pp 101 - 109

[13] Hyunjin Lee, Joonho Gil, and Hyungcheol Shin, "Optimization of Symmetric Spiral Inductors On Silicon Substrate", *IEEE. Trans Microwave*

[14] M. Danesh J. Long, "Differentially driven symmetric microstrip inductors," *IEEE on Microwave theory and techniques,* Vol. 50, No 1 January 2002

[15] S. Michelis, F. Faccio, M. Kayal "Inductor based switching DC-DC converter for low voltage power distribution in SLHC," *TWEPP conference*, Prague, 2007